

Performance Analysis of Limited Bandwidth Active Suspension with Preview Based on a Discrete Time Model

ZHANG XIN, ZHANG JIANWU

School of Mechanical Engineering

Shanghai Jiaotong University

800 Dongchuan Road, Min Hang, Shanghai, 200240

P. R. CHINA

zhangxinmt@163.com

Abstract: - A car suspension system is the mechanism that physically separates the car body from the wheels of the car. Active suspensions differ from the conventional passive suspensions in their ability to inject energy into the system, which can improve the trade-off between the ride comfort and road handling. A discrete optimal control algorithm is proposed in this paper for a limited bandwidth active suspension, in which both look-ahead and wheelbase preview information are utilized. The preview optimal algorithm is implemented in Matlab/Simulink software environment based on a half-vehicle model. The effect of preview time on system performance is investigated. In order to reduce the energy consumption, the effect of various bandwidth of actuator is particularly examined. Simulation results show that the preview time can influence overall system performance remarkably, and 0.2 s look-ahead preview time is preferable. Theoretical deviation of the optimal control gain is given to explain the fact that only look-ahead preview benefits the front wheel's motion while wheelbase preview benefits the rear wheel's motion much more. The pitch motion performance deterioration compared with passive case brought by preview can be eliminated to some extent. With preview information, suspension working space requirement can be restrained to a prominent low degree. 6 Hz system is the most suitable one to achieve the trade-off between performance potential and energy consumption in the range 3~15 Hz for limited bandwidth active suspension.

Key-Words: - Active Suspension, Preview, Control Algorithm, Half-vehicle Model, Limited Bandwidth

1 Introduction

Over the past two decades, numerous published works could be found which focus on active suspension (AS) because of the available potential for vehicle performance improvements [1]. Nevertheless, few successful commercial implementations of AS system are reported. The high cost, complexity, coupled with high energy consumption restricted the development for fully AS systems in which the actuator response frequency range is not limited [2].

Relevantly, limited bandwidth or "slow" active suspension became more attractive than fully AS system and can be a practical alternative for the market because of its potential to achieve similar performance but with much lower cost and energy demand and less problems encountered in fully AS system case. Nissan Infiniti Q45 and Toyota Celica are two typical examples among the early practical applications [3] and [4].

If preview information of road irregularity is

available, the control procedure in active suspension will be more effective and more performance improvement can be expected. Combined with preview information, Berder (1968) first applied stochastic linear optimal control theory to the design of quarter car active suspension system [5]. The work carried out later by Tomizuka showed that much performance benefit can be obtained from the preview information sensed by the sensor mounted at the bumper about 0.8~1m ahead of the front wheel[6]. Although it is argued that preview information is not always reliable, e.g. in the case of obstacle which might be a brick or an empty milk box, the wheelbase preview information sensed by front wheel is truly available for rear wheel in straight, hard road surface running condition, therefore, many relevant research works were carried out recently, but most of them focused either on wheelbase or on look-ahead preview. The former comes from the fact that the rear wheel road input is a time delayed replica of the front; the latter involves using a height

sensor looks ahead of the front wheels road profile [7].

But if both wheelbase and look-ahead preview information can be used, more benefit can be gotten. Sharp, firstly extended the previous work to include both look-ahead and wheelbase preview in a half-car model in which Pade approximation is used to simulate the time delay for the continuous time problem [8] and [9].

However, for any practical implementation of active control system, a discrete time approach for the design problem is more doable for digital control. In fact, any kind of control algorithm should be discretized in the hardware implementation finally. Since the wheelbase of a vehicle is fixed while the speed can be changeable, the controller parameters, such as preview time, sampling frequency, etc. might need to be adapted. On the other hand, the problems in continuous time realization are that Pade representation is imperfect and the realization of the system in practice may not be straightforward [10]. Therefore, a discrete time algorithm using preview information to investigate the effect in the optimization of the slow active suspension is needed.

Taking an off-high military vehicle as example, this paper is concerning on how and why the look-ahead and wheelbase preview together can affect the optimization of the slow-active suspension. In the present study, besides vibration-isolation capability for ride performance along with handling stability, energy consumption is also of vital concern. So, a configuration of slow active suspension is proposed hereby and a standard discrete time linear quadratic regulator (LQR) control algorithm is designed based on a 4-DOF half-vehicle model. In order to keep generality, the results in the following discussion are obtained in a way that efforts are put to eliminate the variety caused by different choices of weighting constants in the LQR design.

2 System modeling

A half-vehicle model with limited bandwidth actuators for the suspension is used throughout the paper. In accordance with the reality, filtered white noise is used as road displacement input, and the rear wheel input is simply a time-delayed version of the front.

Usually, for “slow” active suspension, the limited bandwidth actuator is mounted in series with a conventional spring and thus a damper is mounted in parallel with this combination. Sharp et al gave the reasons for that arrangement, one of which is that at the frequency range beyond the bandwidth of actuator, the system is a conventional passive one, so

unfamiliar difficulties from NVH (Noise, Vibration and harshness) problems will not arise [11].

2.1 Half car model

The scheme of the limited bandwidth half vehicle model is shown in Fig. 1, in which both two kinds of preview are incorporated. The command signal is first fed through two identical second-order low pass filters then to each ideal displace-control actuator in series with suspension spring for limited bandwidth. Two filters instead of one are preferable for the actuator’s behavior at the wheel-hop mode [9].

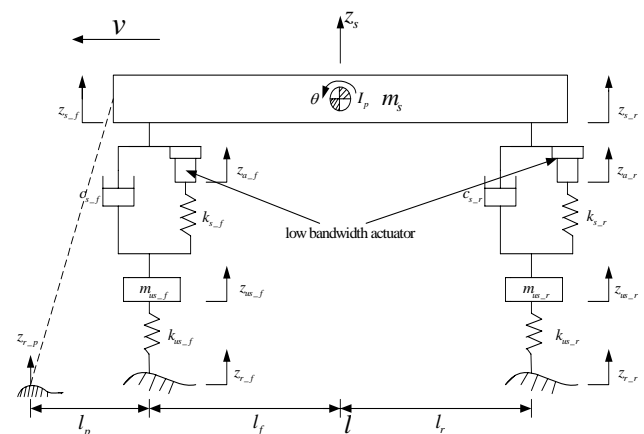


Fig. 1 Half car model with slow suspension actuators

The equations of motion for the suspension model can be written as follows:

$$\left\{ \begin{array}{l} m_s \ddot{z}_s = k_{s-f}(z_{us-f} - z_{a-f}) + c_{s-f}(\dot{z}_{us-f} - \dot{z}_{s-f}) \\ \quad + k_{s-r}(z_{us-r} - z_{a-r}) + c_{s-r}(\dot{z}_{us-r} - \dot{z}_{s-r}) \\ I_p \ddot{\theta} = [k_{s-f}(z_{a-f} - z_{us-f}) + c_{s-f}(\dot{z}_{s-f} - \dot{z}_{us-f})]V_f \\ \quad - [k_{s-r}(z_{a-r} - z_{us-r}) + c_{s-r}(\dot{z}_{s-r} - \dot{z}_{us-r})]V_r \\ m_{us-f} \ddot{z}_{us-f} = c_{s-f}(\dot{z}_{s-f} - \dot{z}_{us-f}) + k_{s-f}(z_{a-f} - z_{us-f}) \\ \quad - k_{us-f}(z_{us-f} - z_{r-f}) \\ m_{us-r} \ddot{z}_{us-r} = c_{s-r}(\dot{z}_{s-r} - \dot{z}_{us-r}) + k_{s-r}(z_{a-r} - z_{us-r}) \\ \quad - k_{us-r}(z_{us-r} - z_{r-r}) \end{array} \right. \quad (1)$$

Where, m_s is sprung mass; z_s is vertical displacement of sprung mass at Center of Gravity; I_p is pitch movement inertia; θ is pitch angle at the center of gravity; m_{us-f}, m_{us-r} are unsprung mass of front and rear wheel respectively; k_{s-f}, k_{s-r} are suspension stiffness of front and rear wheel respectively; k_{us-f}, k_{us-r} are unsprung equivalent stiffness of front

and rear wheel respectively; C_{s_f}, C_{s_r} are suspension equivalent damping of front and rear wheel respectively; l_f, l_r are distance from front and rear suspension to the CG respectively; z_{a_f}, z_{a_r} are output displacement of suspension actuator of front and rear wheel respectively; z_{s_f}, z_{s_r} are vertical displacement of sprung mass connecting to front and rear suspension of front and rear wheel respectively; z_{us_f}, z_{us_r} are vertical displacements of unsprung mass of front and rear wheel respectively; z_{r_f}, z_{r_r} are road irregularity input of front and rear wheel respectively.

Assuming the pitch angle is small, we have:

$$\begin{cases} z_{s_f} = z_s - l_f \theta \\ \dot{z}_{s_f} = \dot{z}_s - l_f \dot{\theta} \\ z_{s_r} = z_s + l_r \theta \\ \dot{z}_{s_r} = \dot{z}_s + l_r \dot{\theta} \end{cases} \quad (2)$$

The filters to limit the actuator bandwidth are standard second order low-pass filters, expressed as:

$$\begin{cases} \frac{z_{s_f}(s) - z_{a_f}(s)}{U_f'(s)} = \frac{U_f'(s)}{U_f(s)} = \frac{\omega_n^2}{s^2 + 2\zeta\omega_n s + \omega_n^2} \\ \frac{z_{s_r}(s) - z_{a_r}(s)}{U_r'(s)} = \frac{U_r'(s)}{U_r(s)} = \frac{\omega_n^2}{s^2 + 2\zeta\omega_n s + \omega_n^2} \end{cases} \quad (3)$$

where U_f, U_r are the command signals for the front and rear suspension actuator; U_f', U_r' are the intermediate variables between the two identical filters with the cut-off frequency ω_n , damping ratio ζ each side; $z_{s_f} - z_{a_f}, z_{s_r} - z_{a_r}$ are respectively the actual relative displacements of the actuators without response delay.

The road excitation model is written as:

$$\begin{cases} \dot{z}_{r_f} = -2\pi f_0 z_{r_f} + 2\pi \sqrt{G_0 v} w_f \\ \dot{z}_{r_r} = -2\pi f_0 z_{r_r} + 2\pi \sqrt{G_0 v} w_r \end{cases} \quad (4)$$

where w_f, w_r are road velocity input white noise signals with unity variance. The low-cutoff frequency f_0 and constant $2\pi \sqrt{G_0 v}$ are used to guarantee a reasonable road displacement power spectral density (PSD), which is approximated by:

$$S(f) = \frac{G_0 v}{f^2} \quad (5)$$

where G_0 is road roughness measured at the reference spatial frequency (wave number), $n_0 = 0.1$ cycles/m. v is the vehicle forward speed, $f_0 = vn_0$.

Defining the state variables as:

$$\begin{aligned} x &= [x_1 \sim x_{18}]^T \\ x_1 &= z_s, x_2 = z_{us_r}, x_3 = z_{us_r} \\ x_4 &= z_{s_f} - z_{a_f}, x_5 = z_{s_r}, x_6 = \theta' \\ x_7 &= \dot{x}_1, x_8 = \dot{x}_2, \dots, x_{12} = \dot{x}_6 \\ x_{13} &= u_f', x_{14} = u_r', x_{15} = \dot{x}_{13}, x_{16} = \dot{x}_{14} \\ x_{17} &= \dot{z}_{r_f}, x_{18} = \dot{z}_{r_r} \end{aligned}$$

The equations of motion for the system can be rewritten into the state space form:

$$\begin{aligned} \dot{x}(t) &= Ax(t) + Bu(t) + Gz_r(t) \\ y(t) &= C_p x(t) + D_p u(t) \end{aligned} \quad (6)$$

where, $z_r(t) = [w_f(t) \ w_r(t)]^T$,

$$u(t) = [u_f(t) \ u_r(t)]^T$$

The discrete-time description of the system dynamics can be written as follows:

$$x(k+1) = \Phi x(k) + \Gamma_u u(k) + \Gamma_i z_r(k) \quad (7)$$

where

$$\Phi = e^{AT_s}, \Gamma_i = \left(\int_0^{T_s} e^{A\eta} d\eta \right) G, \Gamma_u = \left(\int_0^{T_s} e^{A\eta} d\eta \right) B,$$

and

$$\Gamma_i = [\Gamma_{i_f} \ \Gamma_{i_r}]_{18 \times 2}, \Gamma_u = [\Gamma_{u_f} \ \Gamma_{u_r}]_{18 \times 2}$$

2.2 Road preview model

As shown in Fig. 1, denoting the look-ahead preview distance as l_p , because the road input for the front wheel is a delayed version of the look-ahead road profile z_{r_p} with delay time $t_{p0} = \frac{l_p}{v}$, the additional wheelbase preview time $t_{p1} = \frac{l}{v}$ for the rear wheel can be incorporated, and i.e. the preview time for rear wheel is:

$$t_p = t_{p0} + t_{p1} \quad (8)$$

Thus, the total sampling points for preview need to be determined to the selected sampling time T_s are:

$$N_p = N_{p0} + N_{p1} = \frac{t_{p0}}{T_s} + \frac{t_{p1}}{T_s} \quad (9)$$

In the present study, both the look-ahead and wheelbase preview information are considered as augmented system states in discrete time implementation. The state equation for the preview can be written as follows:

$$z(k+1) = Dz(k) + Ez_{r-p}(k) \quad (10)$$

where

$$D = \begin{bmatrix} 0 & 1 & 0 & \dots & 0 \\ 0 & 0 & 1 & \dots & 0 \\ \dots & \dots & \dots & \dots & 0 \\ 0 & 0 & 0 & 0 & 1 \\ 0 & 0 & 0 & 0 & 0 \end{bmatrix}, E = \begin{bmatrix} 0 \\ 0 \\ \dots \\ 0 \\ 1 \end{bmatrix}$$

$$z(k) = [z_1(k) \quad z_2(k) \quad \dots \quad z_{N_p}(k)]^T,$$

$$z_i(k) = z_{r-p}(k - (N_p - i + 1)), i = 1, \dots, N_p.$$

The road input for the front and rear wheel is:

$$z_r(k) \equiv \begin{bmatrix} z_{r-f}(k) \\ z_{r-r}(k) \end{bmatrix} = \begin{bmatrix} C_f \\ C_r \end{bmatrix} z(k) \quad (11)$$

where

$$C_f = [0 \quad \dots \quad 0 \quad 1 \quad \dots \quad 0]_{1 \times N_p},$$

$$C_r = [1 \quad 0 \quad \dots \quad 0]_{1 \times N_p}$$

Combing equation (7), equation (10) with equation (11), and the augmented system with road preview information plus limited bandwidth actuators is obtained:

$$\bar{x}(k+1) = \bar{\Phi}\bar{x}(k) + \bar{\Gamma}_u u(k) + \bar{\Gamma}_i z_{r-p}(k) \quad (12)$$

where $\bar{x}(k) = \begin{bmatrix} x(k) \\ z(k) \end{bmatrix}$,

$$\bar{\Phi} = \begin{bmatrix} \Phi & H \\ 0 & D \end{bmatrix}, \bar{\Gamma}_u = \begin{bmatrix} \Gamma_u \\ 0 \end{bmatrix}, \bar{\Gamma}_i = \begin{bmatrix} 0 \\ E \end{bmatrix}$$

and

$$H = \Gamma_i \begin{bmatrix} C_f \\ C_r \end{bmatrix} = \begin{bmatrix} \overbrace{\Gamma_{i-r}}^{N_{p1}} & 0 & \dots & \overbrace{\Gamma_{i-f}}^{N_{p0}} & 0 & \dots \end{bmatrix}_{18 \times N_p}$$

3 Discrete time optimal control algorithm

Like the continuous time case, the discrete time optimal control problem can be formulated as finding the state feedback gain matrix K_r from the minimization of the cost index function J :

$$J = E\{q_1(z_{is-f} - z_{r-f})^2 + q_2(z_{is-r} - z_{r-r})^2 + q_3\theta^2 + q_4(z_{s-f} - z_{is-f})^2 + q_5(z_{s-r} - z_{is-r})^2 + q_6 z_s^2 + r_1 u_f^2 + r_2 u_r^2\} \quad (13)$$

where $q_1 \dots q_6, r_1, r_2$ are weighting coefficients for performance specifications: handling (q_1, q_2); ride comfort (pitching, q_3 , acceleration at CG of body, q_6); suspension working space (q_4, q_5) and the actuator displacement (r_1, r_2) with fixed value of 1.

The selection of the weighting constants q_i started from such a choice that each component makes an equal contribution to the cost index J [12]. Then, with this base set of q_i , one can iteratively increase some values of these constants to put emphasis on the corresponding performance objectives. For instance, if the ride comfort (vertical acceleration at CG) and dynamic tire deflection are concerned, values of q_1, q_2, q_6 will be increased by a factor of 10. In the remaining of this paper, all the weighting constants are selected based on the above approach.

In discrete time case, the cost index can be expressed as:

$$J = \lim_{N \rightarrow \infty} \frac{1}{N+1} E\{\sum_{k=0}^N (x^T(k)Q_0 x(k) + x^T(k)S_0 u(k) + u(k)S_0^T x(k) + u(k)^T R_0 u(k))\} \quad (14)$$

Where Q_0, R_0 and S_0 are the weighting matrices.

In terms of the augmented state space, the index function can be written as follows:

$$J = \lim_{N \rightarrow \infty} \frac{1}{N+1} E \left[\sum_{k=0}^N x^T(k) \ z^T(k) \begin{bmatrix} Q_0 & 0 \\ 0 & 0 \end{bmatrix} \begin{bmatrix} x(k) \\ z(k) \end{bmatrix} + \begin{bmatrix} x^T(k) & z^T(k) \end{bmatrix} \begin{bmatrix} S_0 \\ 0 \end{bmatrix} u(k) + u^T(k) \begin{bmatrix} S_0^T & 0 \end{bmatrix} \begin{bmatrix} x(k) \\ z(k) \end{bmatrix} + u^T R u \right] \quad (15)$$

Then, the optimal control law can be obtained by the following equation:

$$u = \begin{bmatrix} u_f(k) \\ u_r(k) \end{bmatrix} = -K_r \bar{x}(k) = - \begin{bmatrix} k_{rx} & k_{rz} \end{bmatrix} \begin{bmatrix} x(k) \\ z(k) \end{bmatrix} \quad (16)$$

Where the optimal control gain K_r is calculated by solving a Discrete Algebraic Riccati Equation related to Q_0, R_0 and S_0 , derived as:

$$\begin{cases} k_{rx} = L \left[\Gamma_u^T p_{11} \Phi + S_0^T \right] \\ k_{rz} = L \Gamma_u^T \left[p_{11} H + p_{12} D \right] \end{cases} \quad (17)$$

where $L = \left[\Gamma_u^T p_{11} \Gamma_u + R_0 \right]^{-1}$ and p_{11}, p_{12} are two solutions of the Algebraic Riccati Equation:

$$p_{11} = \Phi^T p_{11} \Phi + Q_0 - (\Phi^T p_{11} \Gamma_u + S_0) L^{-1} (\Gamma_u^T p_{11} \Phi + S_0^T) \quad (18)$$

$$p_{12} = \Phi^T p_{11} H + \Phi^T p_{12} D - k_{rx}^T \Gamma_u^T p_{11} H - k_{rx}^T \Gamma_u^T p_{12} D \quad (19)$$

Noticing $\Phi_c = \Phi - \Gamma_u k_{rx}$, so:

$$p_{12} = \Phi_c^T p_{11} H + \Phi_c^T p_{12} D. \quad (20)$$

In order to study the effect of the preview information in discrete LQR optimal control, one should take a further look inside the state feedback gain k_{rz} in equation (16). Consider the row and column number of Φ_c, H, p_{12} can be rewritten as following equation:

$$p_{12} = \begin{bmatrix} p_1 & p_2 & \dots & p_{N_p} \end{bmatrix} \quad (21)$$

where each p_i is a 18×1 vector.

From equation (10), equation (12), substitute H, D into equation (19) and consider equation (20), the following equation is gotten:

$$\begin{bmatrix} p_1 & p_2 & \dots & p_{N_p} \end{bmatrix} = \Phi_c^T p_{11} \begin{bmatrix} \Gamma_{i,r} & 0 & \dots & \overbrace{\Gamma_{i,f}}^{N_0} & 0 & \dots \end{bmatrix} + \Phi_c^T \begin{bmatrix} 0 & p_1 & \dots & p_{N_p-1} \end{bmatrix} \quad (22)$$

Hence,

$$p_{12} = \begin{bmatrix} \Phi_c^T a & (\Phi_c^T)^2 a & \dots & (\Phi_c^T)^{N_0} a & (\Phi_c^T)^{N_0+1} a + \Phi_c^T b & \dots & (\Phi_c^T)^{N_p} a + (\Phi_c^T)^{N_p} b \end{bmatrix} \quad (23)$$

where $a = p_{11} \Gamma_{i,r}, b = p_{11} \Gamma_{i,f}$, implying that p_{12} can be only represented in terms of p_{11} and the optimized closed-loop system dynamics.

Let $\Delta_i = (\Phi_c^T)^i p_{11}, i = 0, 1, \dots, N_p$ and consider $\Gamma_u = \begin{bmatrix} \Gamma_{u,f} & \Gamma_{u,r} \end{bmatrix}$, then,

$$k_{rz} = L \Gamma_u^T \left[p_{11} H + p_{12} D \right] = L \begin{bmatrix} \Gamma_{u,f}^T \Delta_0 \Gamma_{i,r}, \Gamma_{u,f}^T \Delta_1 \Gamma_{i,r}, \dots, \Gamma_{u,f}^T \Delta_{N_p-1} \Gamma_{i,r}, \\ \Gamma_{u,r}^T \Delta_0 \Gamma_{i,r}, \Gamma_{u,r}^T \Delta_1 \Gamma_{i,r}, \dots, \Gamma_{u,r}^T \Delta_{N_p-1} \Gamma_{i,r}, \\ \Gamma_{u,f}^T \Delta_{N_0} \Gamma_{i,r} + \Gamma_{u,f}^T \Delta_0 \Gamma_{i,f}, \dots, \Gamma_{u,f}^T \Delta_{N_p-1} \Gamma_{i,r} + \Gamma_{u,f}^T \Delta_{N_0-1} \Gamma_{i,f} \\ \Gamma_{u,r}^T \Delta_{N_0} \Gamma_{i,r} + \Gamma_{u,r}^T \Delta_0 \Gamma_{i,f}, \dots, \Gamma_{u,r}^T \Delta_{N_p-1} \Gamma_{i,r} + \Gamma_{u,r}^T \Delta_{N_0-1} \Gamma_{i,f} \end{bmatrix} \quad (24)$$

In the obtained k_{rz} , the first row of k_{rz} can be treated as the optimal feedback gain carrying the sensed road information fed to the front actuator; the second row is the corresponding one which is fed to the rear actuator.

In the quarter car case as [7],

$$k_{rz} = L \begin{bmatrix} \Gamma_u^T \Delta_0 \Gamma_i, & \Gamma_u^T \Delta_1 \Gamma_i, & \dots & \Gamma_u^T \Delta_{N_p} \Gamma_i \end{bmatrix} \quad (25)$$

For the benefits from preview, the optimal control law shows that the road input Γ_i should be coupled with corresponding command input channel Γ_u in optimal state feedback gain, which is not a problem in the quarter case, a single-input system. While in the half car system, from equation (24), the road input is not always connected to the corresponding command input channel in the state feedback gain.

4 Result analysis

With the increase of vehicle forward speed, the performance improvement from wheelbase preview becomes less since wheelbase preview time is shortened correspondingly. But for look-ahead preview, by changing the amount of preview distance, one can maintain a constant preview time even though the forward speed changes. Comparing with passive case, the slow-active suspension shows significant performance improvement from both wheelbase and look-ahead preview. Simulations are carried out to investigate the following aspects:

- The performance comparison between

passive suspension, slow-active suspension with and without preview in 4 objectives: 1) Vertical motion at C.G; 2) Pitch motion; 3) Dynamic tire deflection and 4) Suspension working space.

- The same comparison between the slow-active suspensions with various preview time. All of them have at least 0.16 s wheelbase preview time.
- The energy consumption comparison between different actuator bandwidth in slow-active suspension.

All of the results are obtained based on a constant vehicle speed at 20 m/s and structure parameters are listed in Table 1. The bandwidth for slow active suspension for item 1 and 2 is selected to be 6 Hz.

Table 1 Structure parameter values

Parameter	Value
Sprung mass , m_s	5630 kg
Unsprung mass of front wheel, m_{us_f}	600 kg
Unsprung mass of rear wheel, m_{us_r}	650 kg
Suspension stiffness of front wheel, k_{s_f}	3.5×10^5 N/m
Suspension stiffness of rear wheel, k_{s_r}	3.5×10^5 N/m
Unsprung equivalent stiffness of front wheel, k_{us_f}	2.5×10^5 N/m
Unsprung equivalent stiffness of rear wheel, k_{us_r}	2.6×10^5 N/m
Suspension equivalent damping of front wheel, C_{s_f}	19000 Ns/m
Suspension equivalent damping of rear wheel, C_{s_r}	16500 Ns/m
Pitch movement inertia, I_p	12000 kgm^2
Distance from front suspension to the CG, l_f	1.85 m
Distance from rear suspension to the CG, l_r	1.35 m
Distance of look-ahead preview, l_p	0~6 m
Road roughness coefficient, G_0	6.4×10^{-5} m^3
Vehicle forward speed, v	20 m/s

4.1 Performance comparison between different suspension structures

Firstly, performances are compared between

conventional passive suspension, slow-active system without any kind of preview and slow-active system with 0.2 s look-ahead plus 0.16 s wheelbase preview time. Fig. 2 shows the performance comparison of vertical acceleration at CG, it implies that with appropriate look-ahead preview, 6 Hz slow-active system can achieve very satisfactory improvement compared with the passive and non-preview case and has the potential to control the wheel hop mode.

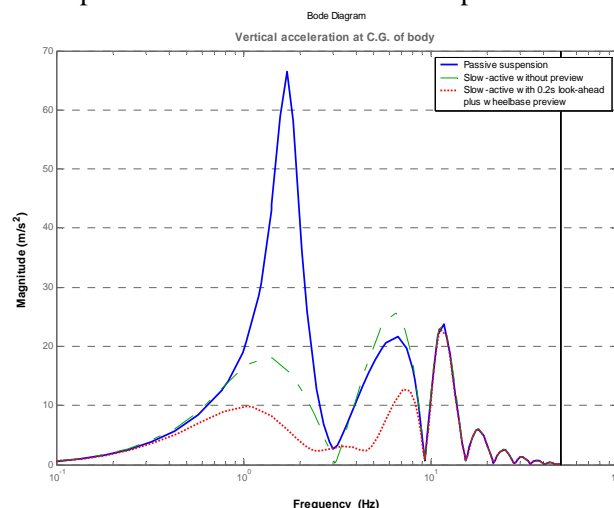


Fig. 2 Comparison in body vertical acceleration between 3 kinds of slow-active suspensions

As shown in Fig. 3, the similar result can be obtained in pitch motion case, while for other types of vehicle, the benefit from preview information might not be so significant. The coupling effect from the fact $m_s l_f l_r \neq I_p$ and “wheelbase-filtering” effect complicate the pitch motion to some extent.

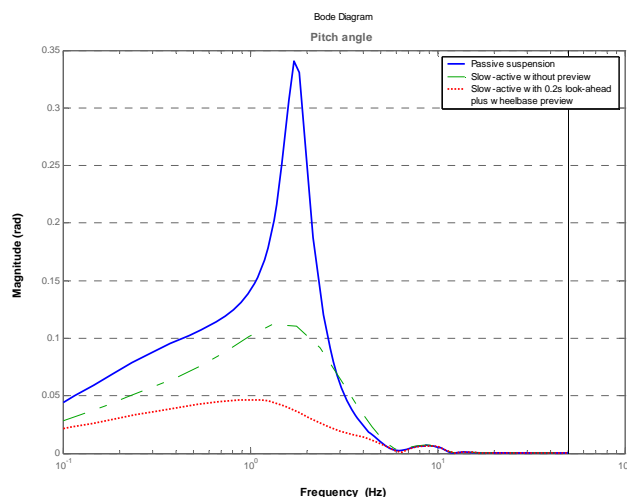
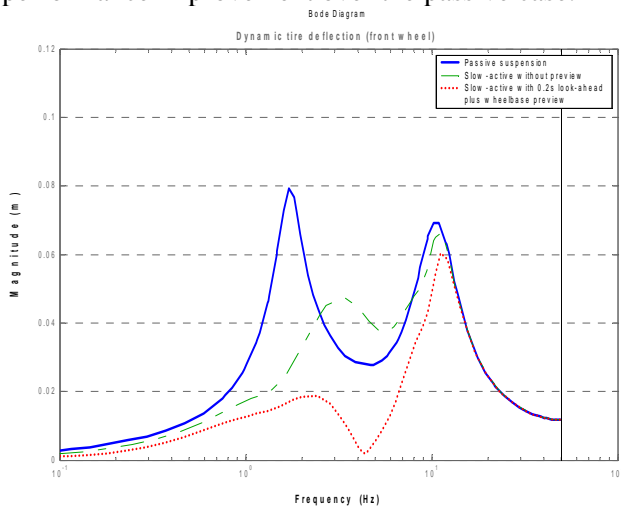


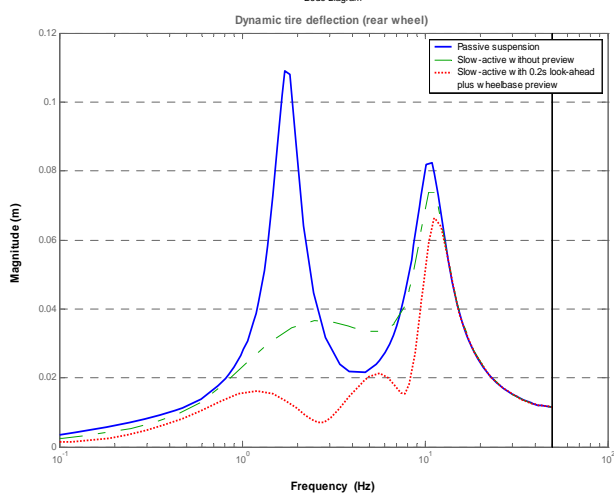
Fig. 3 Comparison in the pitch angle between 3 kinds of slow-active suspensions

The performance comparison of dynamic tire deflection is shown in Fig. 4. In fact, the contribution of look-ahead preview to front wheel is almost the

same as the contribution of wheelbase preview to rear wheel, and both of them have a significant performance improvement over the passive case.



(a)

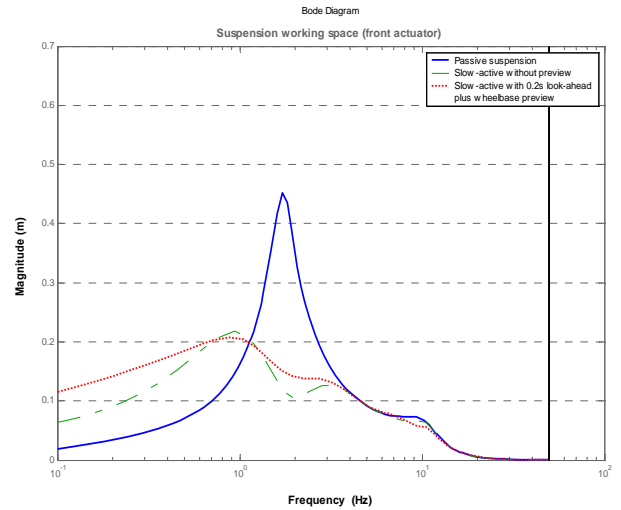


(b)

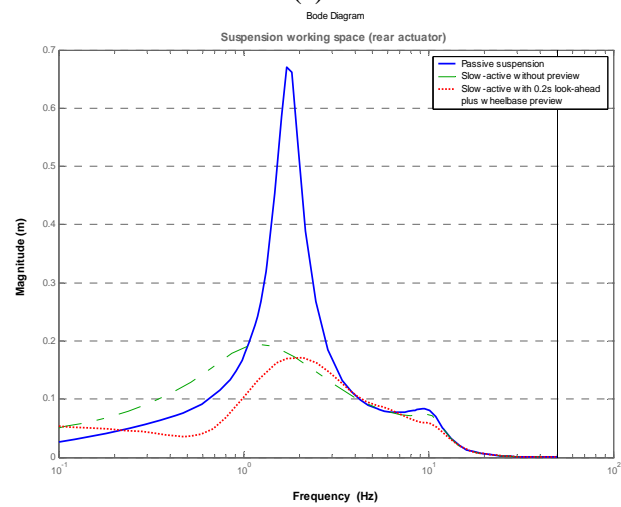
Fig. 4 Comparison in dynamic tire deflection between 3 kinds of slow-active suspensions

(a) front wheel; (b) rear wheel

As shown in Fig. 5, the responses of suspension working space requirements indicate the performance improvement 0.2 s look-ahead preview time brings. Comparing with non-preview slow active or passive cases, working space requirement can also be reduced to a competitively low degree in rear suspension. However, in reality, such a small amount of working space requirement may not be achieved because the working space is also determined by the suspension actual structure and the initial equilibrium relative position between sprung and unsprung mass.



(a)



(b)

Fig. 5 Comparison in suspension working space between 3 kinds of slow-active suspensions

(a) front wheel; (b) rear wheel

4.2 Effects of slow-active suspension with different preview times

Fig. 6 shows results of vertical acceleration at the body CG. It can be seen that 0.3 s look-ahead preview plus 0.16 s wheelbase preview time is sufficient to achieve available benefit and nearly no further performance improvement can be obtained when preview time increases, which is also true for all other aspects.

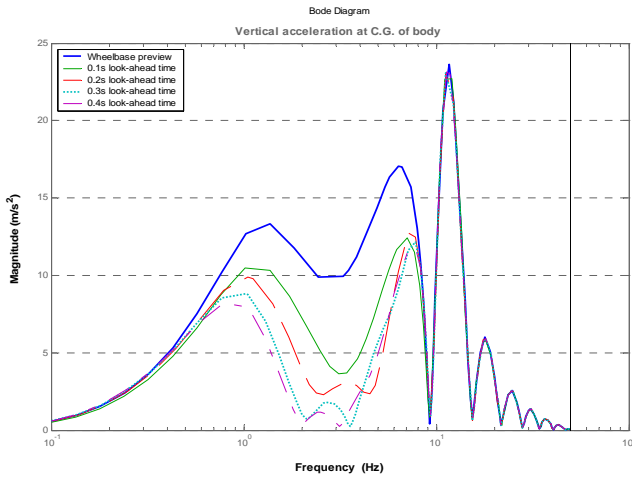


Fig. 6 Vertical acceleration at the body C.G. with different preview times

However, after a significant improvement under 0.1 s look-ahead preview time, the pitch motion’s performance degrades in the range of 0.2 Hz ~ 2 Hz as the preview time increases, which can be seen from Fig. 7. Results from iterations of other sets of weighting constants in cost index equation (13) also imply that even though more preview time is given, equivalent performance benefit at 0.1 s preview time can hardly be achieved without significant deterioration.

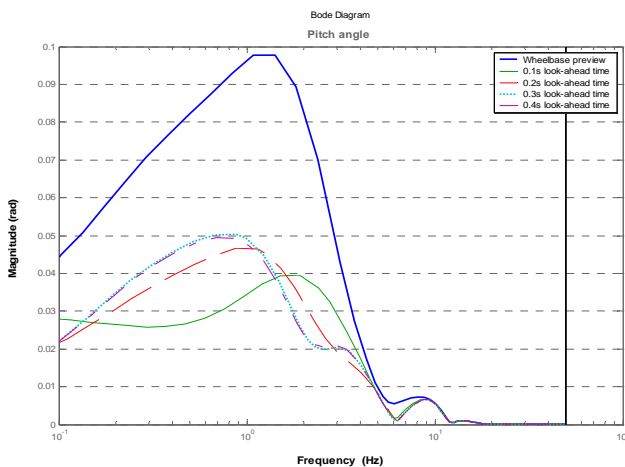
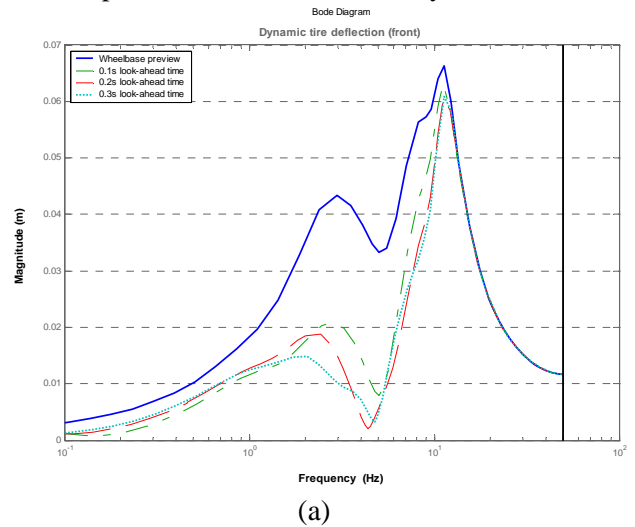


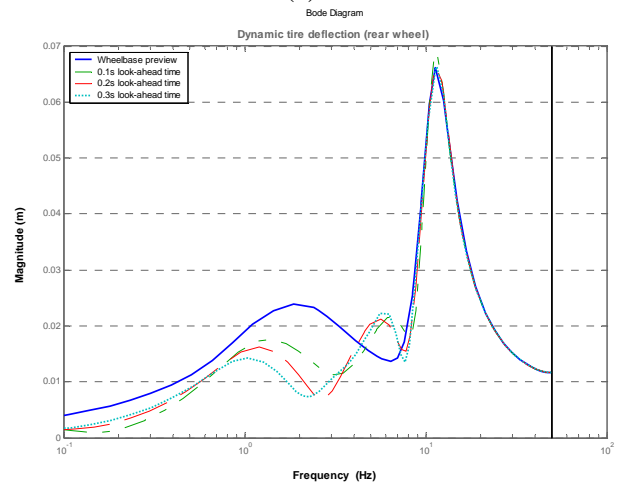
Fig. 7 The pitch angle response with different preview times

The responses of dynamic tire deflection are shown in Fig. 8, implying that 0.2 s look-ahead preview time is preferable for both the front wheel and rear wheel. Because of the existence of wheelbase preview, the rear tire deflection is smaller than the front one, providing zero look-ahead preview time, i.e., wheelbase preview only. RMS values show that with wheelbase preview, the rear wheel has 21.7% reduction in tire deflection comparing with the passive system while the front wheel has 1.6% reduction. If giving the front wheel

0.2 s look-ahead time, 19.0% improvement can be obtained in the front wheel and another 0.6% performance improvement is brought to the rear wheel. In other words, the response of front wheel’s tire deflection gains more benefit than the rear’s from look-ahead preview and the rear tire deflection benefits more from wheelbase preview if both two kinds of preview exist simultaneously.



(a)



(b)

Fig. 8 Tire deflection with different preview times
(a) front wheel; (b) rear wheel

This can be explained by two facts. Firstly, from equation (23), the optimal law from the previewed road information is implemented by taking Φ_c^T the power of i , if $i > 1$, the “slower” modes are emphasized, which means in the beginning of the preview time the optimal law emphasizes on controlling the “slower” modes, whereas “faster” modes are emphasized rather late[13]. So, 0.16 s wheelbase preview time is enough for the rear tire’s wheel hop mode, more look-ahead preview time is no use in that frequency range.

Second, as mentioned before, the road input in

the half car model is not always connected to the corresponding input channel in the optimal state feedback gain. In the first row of equation (24), only the last N_{p0} terms contain $\{\Gamma_{u_{-f}}^T, \Gamma_{i_{-f}}\}$ pair, which means only look-ahead preview time is useful for the optimal control of the front wheel motion; in the second row, the last N_{p0} terms contain $\{\Gamma_{u_{-r}}^T, \Gamma_{i_{-r}}\}$ pairs, which breaches the optimal control law (see equation (25)), so look-ahead preview time can not bring much benefit to the rear wheel.

Fig. 9 shows the frequency responses of the front and rear suspension working spaces. For the front case, 0.3 s preview time and more have a decrease on working space demand compared with 0.2 s preview time. And 0.1 s case requires a surprisingly high amount of working space. The rear suspension is similar to the front case, except that 0.2 s preview time demands much less working space than 0.1 s in the front case.

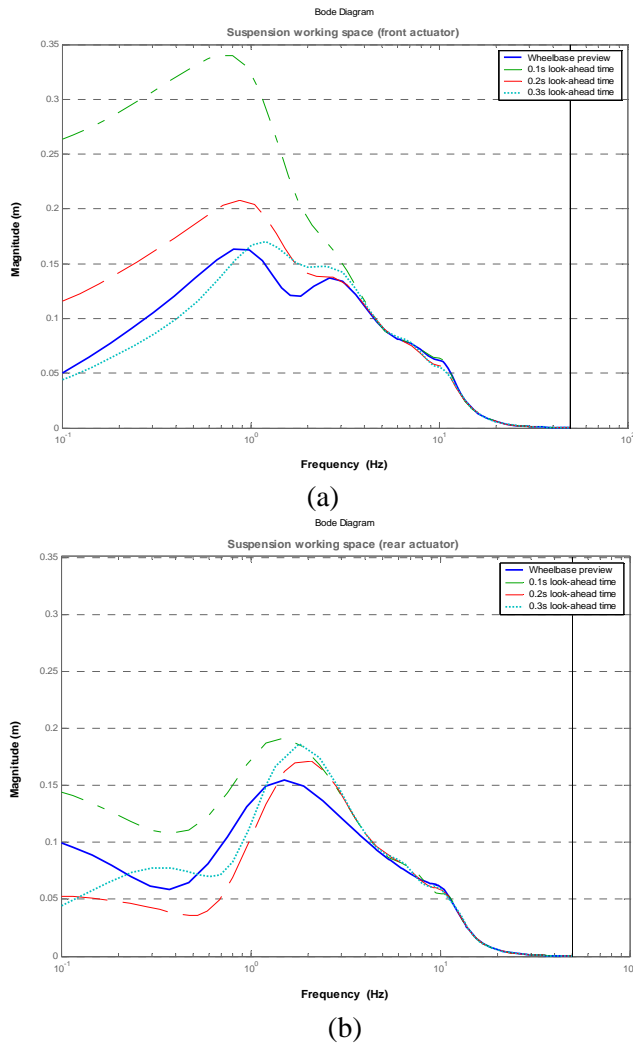


Fig. 9 Suspension working space with different preview times
(a) front actuator; (b) rear actuator

From above all, in consideration of all the components' response, 0.2 s can be chosen as a suitable look-ahead preview time since the best compromise of performance improvements can be available for the present simulations.

4.3 Energy Consumption

In order to extend the discussion of the improvement in slow-active suspension with preview to a practical point of view, the energy consumption should also be considered. Using the intuitionistic method proposed by Pilbeam et al, one can get the relation between energy consumption of slow-active suspension and preview time for different bandwidth[14]. The method is summarized as follows (front actuator, for instance; the rear actuator case is totally the same):

The total energy consumed in the time range $0 \sim t_{sim}$:

$$E_{front} = \frac{1}{2} p_{sup} V = \frac{1}{2} p_{sup} A \int_0^{t_{sim}} |\dot{z}_{s_{-f}} - \dot{z}_{a_{-f}}| dt \quad (26)$$

where p_{sup} is the hydraulic supply pressure, A is actuator's piston cross-sectional area and $\dot{z}_{s_{-f}} - \dot{z}_{a_{-f}}$ is the velocity of the fluid flow. The average power consumption over this period is then given by:

$$P_f = \frac{E_{front}}{t_{sim}} = \frac{p_{sup} A}{2t_{sim}} \int_0^{t_{sim}} |\dot{z}_{s_{-f}} - \dot{z}_{a_{-f}}| dt \quad (27)$$

Average power consumption VS. preview time

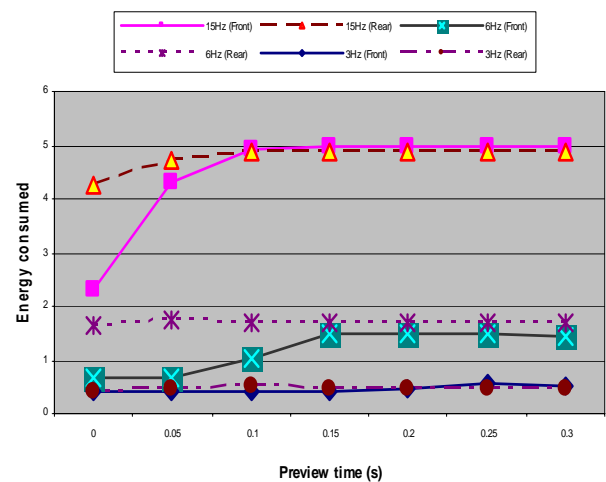


Fig. 10 Power consumption under various preview times

(Zero preview time means wheelbase preview only)

Fig. 10 shows the results for 3 Hz, 6 Hz and 15 Hz actuator bandwidth systems with the normalized

value of the term outside the integral in equation (27). Because look-ahead preview affects front suspension more than rear suspension, for the front actuator, higher bandwidth system requires more energy and less preview time to achieve its maximum effort. 15 Hz system reaches its capability limit at 0.1 s preview time and requires 227% more energy than 6 Hz system does at 0.15 s preview time, while for the rear actuator, power consumption does not change much with the increasing preview time.

5 Conclusions

In the study of the slow-active suspension with look-ahead and wheelbase preview for a military engineering vehicle, a discrete time algorithm are designed by using a half vehicle model. The simulation results show clearly the different amount of performance improvement offered by various look-ahead and wheelbase preview times. By comparison, 0.2 s look-ahead preview time is preferable for the overall performance. Although the results are given based on a military vehicle with a comparatively high weight, similar results can be achieved on other types of vehicle such as ordinary saloon car.

Based on previous work, theoretical deviation of the optimal control gain k_{rz} is given to explain the fact that only look-ahead preview benefits the front wheel's motion while wheelbase preview benefits the rear wheel's motion much more.

The pitch motion performance deterioration compared with passive case brought by preview can be eliminated to some extent.

Results also show that with preview information, suspension working space requirement can be restrained to a prominent low degree.

By using a rough and intuitionistic method, it also shows 6 Hz system is the most suitable one to achieve the trade off between performance potential and energy consumption in the range 3~15 Hz for limited bandwidth active suspension.

Acknowledgements

The paper is supported by the National Natural Science Foundation of China (No.50875158) and the National Key Technology R&D Program of China (No.2006BAB11B05).

References:

[1] D. Hrovat, Survey of Advanced Suspension Developments and Related Optimal Control Applications, *Automatica*, Vol. 33. No. 10. 1997,

pp. 1781-1817.

- [2] D. A. Crolla, G. Firth, D. Horton, *An Introduction to Vehicle Dynamics*, School of Mechanical Engineering, University of Leeds, 1992.
- [3] Aoyama Y., Kawabata. K., Hasegawa S. et al, Development of the full active suspension by Nissan, *SAE paper* 901747, 1990.
- [4] Yokoya Y., Kizu R., Kawaguchi H., Integrated control system between active control suspension and four wheel steering for the 1989 Celica, *SAE paper* 901748, 1990.
- [5] Bender E. K., Optimum linear preview control with application to vehicle suspension, *Journal of Basic Engineering*, Vol. 90, 1968, pp. 213-221.
- [6] Tomizuka, M., Optimum linear preview control with application to vehicle suspension –revisited, *Trans. A.S.M.E., J. Dynamic Systems, Measurement and Control*, Vol. 98, 1976, pp. 309-315.
- [7] N. Louam, D. A. Wilson, R. S. Sharp, Optimal Control of a Vehicle Suspension Incorporation the Time Delay between Front and Rear Wheel Inputs, *Vehicle System Dynamics*, Vol. 17, 1988, pp. 317-336.
- [8] Sharp R. S., Pilbeam, C., On the Ride Comfort Benefits available from Road Preview with Slow-active Car Suspensions, *Vehicle System Dynamics*, Vol. 23, Suppl. 1994, pp. 437-448.
- [9] Pilbeam, C., Sharp R. S., On the preview control of limited bandwidth vehicle suspensions, *Proc. I. Mech. E., Part D*, Vol. 207, 1993, pp. 185-193.
- [10] Sharp R.S., Wilson D. A., On control laws for vehicle suspension accounting for input correlations, *Vehicle System Dynamics*, Vol. 19, No. 6, 1990, pp. 353-363.
- [11] Sharp R. S., Hassan S. A., On the performance capabilities of active automobile suspension system of limited bandwidth, *Vehicle System Dynamics*, Vol. 16, 1987, pp. 213-225.
- [12] G. F. Franklin, J. D. Powell, M. Workman, *Digital Control of Dynamic Systems, 3rd edition*, Addison Wesley Longman Inc., 1998.
- [13] Prokop G., Sharp R. S., Performance enhancement of limited bandwidth active automotive suspension by road preview, *IEE Proceedings: Control Theory and Applications*, Vol. 142, No. 2, 1995, pp. 140-148.
- [14] Pilbeam C., Sharp R. S., Performance potential and power consumption of slow-active suspension systems with preview, *Vehicle System Dynamics*, Vol. 25, 1996, pp. 169-183.